

Searching for λ Boo stars in binary systems

J. Alacoria^{1,5}, C. Saffe^{1,2,5}, A. Collado^{1,2,5}, A. Alejo^{1,2,5}, D. Calvo^{1,2,5}, P. Miquelarena^{1,2,5}, E. González², M. Flores^{1,2,5}, M. Jaque Arancibia^{3,4}, and F. Gunella^{1,5}

¹ Instituto de Ciencias Astronómicas, de la Tierra y del Espacio (ICATE-CONICET), C.C 467, 5400, San Juan, Argentina.

² Universidad Nacional de San Juan (UNSJ), Facultad de Ciencias Exactas, Físicas y Naturales (FCEF), San Juan, Argentina.

³ Instituto de Investigación Multidisciplinar en Ciencia y Tecnología, Universidad de La Serena, Raúl Bitrán 1305, La Serena, Chile

⁴ Departamento de Física y Astronomía, Universidad de La Serena, Av. Cisternas 1200 N, La Serena, Chile.

⁵ Consejo Nacional de Investigaciones Científicas y Técnicas (CONICET), Argentina

Received xxx, xxx ; accepted xxx, xxxx

ABSTRACT

Context. The origin of λ Boo stars is currently unknown. Very few of them are known as members of multiple systems, which could provide benchmark laboratories to study their origin.

Aims. Our goal is to find new candidate λ Boo stars that belong to binary systems. Then, a detailed abundance determination of some candidates could confirm their true λ Boo nature, while the composition of eventual late-type companions could be used as a proxy for the initial composition of the λ Boo stars.

Methods. We cross-matched a homogeneous list of candidate λ Boo stars with a recent Gaia eDR3 catalog of resolved binaries. Then, we carried out a detailed abundance determination via spectral synthesis of three of these systems, hosting a candidate λ Boo star and a late-type companion: HD 98069 + UCAC4 431-054639, HD 87304 + CD-33 6615B and HD 153747 + TYC 7869-2003-1. Stellar parameters were estimated by fitting observed spectral energy distributions (SEDs) with a grid of model atmospheres using the online tool VOSA, together with Gaia eDR3 parallaxes and the PARAM 1.3 interface. Then, the abundances were determined iteratively for 31 different species by fitting synthetic spectra using the SYNTH program together with local thermodynamic equilibrium (LTE) ATLAS12 model atmospheres. Specific opacities were calculated for each star, depending on its arbitrary composition and microturbulence velocity, v_{micro} , through the opacity sampling (OS) method. The abundances of the light elements C and O were corrected by non-LTE effects. The complete chemical patterns of the stars were then compared to those of λ Boo stars.

Results. We obtained a group of 19 newly identified binary systems which contain a candidate λ Boo star, allowing to \sim duplicate the number of λ Boo stars currently known in multiple systems. This important group could be used in further studies of λ Boo stars. For the first time, we performed a detailed abundance analysis of three of these binary systems which includes a candidate λ Boo star and a late-type companion. We confirmed the true λ Boo nature of the three early-type stars (HD 87304, HD 98069 and HD 153747), and obtained mostly a solar-like composition for their late-type components. Adopting as a proxy the late-type stars, we showed that the three λ Boo stars were initially born with a solar-like composition. This is an important constraint for any scenario trying to explain the origin of λ Boo stars. The present work provides three numerical examples of possible "starting" and "ending" compositions to test formation models of λ Boo stars. Also, the solar-like composition of the late-type stars supports the idea that λ Boo stars are Population I objects, however, we caution that other explanations are also possible.

Conclusions. We performed, for the first time, a detailed abundance analysis of binary systems including a λ Boo star and a late-type companion. We obtained a solid indication that λ Boo stars born from a solar-like composition and established an important constraint to test formation models of λ Boo stars.

Key words. Stars: abundances – Stars: binaries – Stars: chemically peculiar – Stars: individual: HD 87304, CD-33 6615B, HD 98069, UCAC4 431-054639, HD 153747, TYC 7869-2003-1

1. Introduction

The λ Boo stars are considered as one of the long-standing puzzles in astrophysics. They are a rare class of stars, making up about $\sim 2\%$ of the population of stars of spectral type A (Gray & Corbally 1998; Paunzen et al. 2001b). The main characteristic of λ Boo stars is a notable surface depletion of most Fe-peak elements together with near-solar abundances of lighter elements C, N, O, and S (e.g. Kamp et al. 2001; Andrievsky et al. 2002; Heiter et al. 2002; Alacoria et al. 2022). The origin of the λ Boo peculiarity remains a challenge despite recent efforts (see e.g. Jura 2015; Kama et al. 2015; Murphy & Paunzen 2017; Kunitomo et al. 2018; Saffe et al. 2021; Alacoria et al. 2022). The scenarios trying to explain the notable abundance pattern point to diverse ideas, including accretion of gas from a circum-

stellar disk (Venn & Lambert 1990), the ingestion of comets and volatile-rich objects (Gray & Corbally 2002), the interaction of the star with the interstellar medium (ISM) or with a diffuse interstellar cloud (Cowley et al. 1982; Kamp & Paunzen 2002; Martinez-Galarza et al. 2009), and the ablation of volatile gases from a near hot-Jupiter planet (Jura 2015). However, none of the suggested scenarios seem to explain the origin of the λ Boo stars (see e.g. the recent discussion in Murphy & Paunzen 2017; Alacoria et al. 2022).

The detection of λ Boo stars as members of binary systems is considered an important finding, being a laboratory to test physical conditions under which these stars formed. However, currently few λ Boo stars are clearly identified as members of these systems. For example, Paunzen et al. (2012a,b) identified a \sim dozen of λ Boo stars as members of early-type binary sys-

tems, and proposed a method to test the accretion scenario. They suggested that two early-type stars passing through a diffuse cloud should display, in principle, the same superficial peculiarity (see also Alacoria et al. 2022). The detection of a binary or multiple system including a λ Boo star and a late-type companion is also valuable. In this case, the chemical composition of the late-type component could be considered as a proxy of the original composition from which both stars formed, being crucial to test formation models of λ Boo stars (e.g. Alacoria et al. 2022). If the composition of the λ Boo and the late-type star differs significantly, this would be a solid indication that the λ Boo was originally born with a different composition. Also, the "differential pattern" between these stars could help to precisely quantify the λ Boo phenomena, that is, to measure element by element the effect produced by the λ Boo peculiarity. However, to our knowledge, only one multiple system including a late-type component is reported in the literature: the remarkable triple system HD 15165 (Alacoria et al. 2022). The examples mentioned show that the detection of multiple systems including a λ Boo component could provide benchmark laboratories, being an important tool to study the origin of λ Boo stars.

Progress in understanding the λ Boo stars has been hindered by a somewhat heterogeneous literature (see e.g. section 1.2 in Murphy et al. 2015). This motivated to reevaluate the membership of previously reported λ Boo stars (see Murphy et al. 2015; Gray et al. 2017; Murphy et al. 2020), using mainly classification spectroscopy. Together, these three works comprise a complete and homogeneous sample of predominantly southern λ Boo stars. On the other hand, El-Badry et al. (2021) recently obtained an extensive catalog of 1.3 (1.1) million of spatially resolved binaries with a bound probability $>90\%$ ($>99\%$) within ~ 1 kpc of the Sun, using Gaia eDR3 data. We caution that 15% of A-type stars have companions with periods of 100–1500 days (Murphy et al. 2018), which would be undetected in the El-Badry et al. (2021) study. Then, with the aim of detect λ Boo stars in multiple systems, we cross-matched the compilation of 118 λ Boo stars with this recent catalog of resolved binaries. The results of this experiment are presented in the Table 1, showing a list of λ Boo stars together with their corresponding binary companions. The columns present the binary number, star name, V magnitude, coordinates J2016.0 (α and δ), proper motions (μ_α and μ_δ), parallax π , and finally separation (in seconds and au). As previously explained, this important group of newly identified binary systems could be used in further studies of λ Boo stars. Most λ Boo stars of Table 1 have late-type companions. The binaries include separations ranging between ~ 150 au up to ~ 57000 au. We note that the list includes one binary system (the number 7, HD 198160/HD 198161) having a previously known λ Boo star candidate (Gray 1988; Stürenburg 1993; Alacoria et al. 2022).

We present in this work, the first detailed analysis of binary systems which include a candidate λ Boo star and a late-type companion. We focused on three relatively bright binary systems included in the Table 1, obtaining fundamental parameters and abundances for their components. The separation of the stars allowed us to obtain clean individual spectra, free from a possible contamination from its stellar companion. This will allow us to determine, for the first time, a solid proxy for the starting chemical composition of the λ Boo stars, that is, the chemical composition from which the λ Boo stars born. This is a critical constraint for any model that explains the origin of λ Boo stars. In addition, the stars analyzed together with those presented in the Table 1, are important laboratories for further studies of λ Boo stars. The new binary systems reported in Table 1 allow to \sim duplicate the

number of λ Boo stars currently known in multiple systems. The sample could also help to determine if the presence of an stellar companion could play a role in the development of the peculiarity.

This work is organized as follows. In Sect. 2, we describe the observations and data reduction. In Sect. 3, we present the stellar parameters and chemical abundance analysis. In Sect. 4, we show the results and discussion. Finally, in Sect. 5, we highlight our main conclusions.

2. Observations

We present in Table 2 the visual magnitude V, coordinates, proper motions, parallax and signal-to-noise per pixel (~ 5000 Å), for the stars studied in this work. The spectral data of the binary system HD 87304 + CD-33 6615B were acquired through the Gemini High-resolution Optical SpecTrograph (GHOST), which is attached to the 8.1 m Gemini South telescope at Cerro Pachón, Chile. GHOST is illuminated via 1.2" integral field units that provide the input light apertures. The spectral coverage of GHOST between 360–900 nm is appropriate for deriving stellar parameters and chemical abundances using several features. It provides a high resolving power $R \sim 50000$ in the standard resolution mode¹. The read mode was set to medium, as recommended for relatively bright targets. The observations were taken on October 10, 2024 and October 24, 2024 (PI: Carlos Saffe, Program ID: GS-2024B-Q-403) using the same spectrograph configuration for both stars. The exposure times were 120 sec and 1100 sec (for HD 87304 and CD-33 6615B), obtaining a final signal-to-noise ratio (S/N) between ~ 220 –275 per pixel measured at ~ 5000 Å for both stars. The spectra were reduced using the GHOST data reduction pipeline v1.1.0, which works under DRAGONS². This is a platform for the reduction and processing of astronomical data.

The spectra of the binary systems HD 98069 + UCAC4 431-054639 and HD 153747 + TYC 7869-2003-1 were obtained at the Complejo Astrónomico El Leoncito (CASLEO) during Mar 15-16, 2024, Jun 11-12, 2024 and Jul 11-12, 2024 (PI: José Alacoria, Program ID: JS-2024A-06). We used the *Jorge Sahade* 2.15-m telescope equipped with a REOSC echelle spectrograph³ and a SOPHIA 2048 \times 2048 (152-VS-X eXcelon) CCD detector. The REOSC spectrograph uses gratings as cross-dispersers. We used a grating with 300 lines mm^{-1} (disperser # 270), which provides a resolving power of ~ 13500 or more, covering appropriately a spectral range of λ 3700–7500. Five individual spectra for each object were obtained and then combined, reaching an average S/N per pixel of ~ 235 measured at ~ 5000 Å. We take the stellar spectra for each target followed by a ThAr lamp in order to derive an appropriate pixel versus wavelength solution. The data were reduced with Image Reduction and Analysis Facility (IRAF) following the standard recipe for echelle spectra (i.e., bias and flat corrections, order-by-order normalization, scattered light correction, etc.). The continuum normalization and other operations (such as Doppler correction and combining spectra) were performed using IRAF.

¹ <https://www.gemini.edu/instrumentation/ghost>

² <https://www.gemini.edu/observing/phase-iii/reducing-data/dragons-data-reduction-software>

³ On loan from the Institute d' Astrophysique de Liege, Belgium.

Table 1. Visual binary systems that include a λ Boo star component (the first star listed), identified with Gaia eDR3 data.

Binary number	Star name	V	α	δ	μ_α	μ_δ	π	Sep.	Sep.
			J2016.0	J2016.0	[mas/yr]	[mas/yr]	[mas]	["]	[au]
1	HD 112948	9.35	13 0 42.78	-36 9 5.83	-27.528	-2.159	2.719	24.38	8967.79
	Gaia DR3 6154835886339634304		13 0 44.58	-36 9 16.56	-27.447	-2.160	2.769		
2	HD 91130	5.91	10 31 51.40	+32 22 46.53	16.652	7.876	12.101	38.87	3211.74
	Gaia DR3 748463991961311488		10 31 48.36	+32 22 41.11	16.302	8.891	12.187		
3	HD 107233	7.36	12 19 55.73	-48 18 59.76	50.923	-17.777	12.379	15.02	1213.63
	Gaia DR3 6130179235015300096		12 19 54.22	-48 18 58.99	50.085	-18.487	12.332		
4	HD 319	5.92	0 7 46.98	-22 30 31.37	68.586	-35.437	11.690	1.84	157.43
	HD 319B		0 7 47.06	-22 30 32.87	69.557	-26.724	11.399		
5	HD 153747	7.42	17 2 53.84	-38 27 36.60	7.488	13.836	5.647	322.64	57131.24
	TYC 7869-2003-1	11.84	17 2 38.75	-38 23 7.05	7.604	13.963	5.627		
6	HD 168740	6.12	18 25 31.63	-63 1 19.17	-0.017	-102.405	14.056	65.11	4631.9
	Gaia DR3 6630272406475726592		18 25 40.04	-63 1 50.19	-0.193	-104.575	14.086		
7	HD 198160	6.21	20 51 38.70	-62 25 46.34	82.885	-47.171	13.599	2.44	179.57
	HD 198161		20 51 39.05	-62 25 45.93	82.063	-42.345	13.625		
8	HD 46722	9.29	6 33 46.53	-27 57 21.84	-18.649	0.201	4.590	40.55	8833.78
	Gaia DR3 2895732444923489408		6 33 49.46	-27 57 10.07	-18.687	0.199	4.573		
9	HD 168947	8.11	18 24 30.07	-44 11 56.67	8.242	0.875	3.872	104.64	27022.47
	Gaia DR3 6721717074879155840		18 24 22.47	-44 10 51.32	8.286	0.511	3.815		
10	HD 40588	6.19	6 1 10.02	+31 2 4.27	-20.388	0.307	13.342	29.91	2241.98
	Gaia DR3 3449874691731245184		6 1 8.07	+31 1 47.90	-21.721	-0.135	13.468		
11	HD 75654	6.36	8 49 52.27	-39 8 29.12	-63.354	40.784	13.914	284.08	20417.17
	Gaia DR3 5525846343983205376		8 50 7.45	-39 4 46.68	-62.674	40.545	13.941		
12	HD 87304	9.49	10 3 23.43	-33 41 2.58	-19.776	0.833	2.204	6.97	3160.67
	CD-33 6615B	12.60	10 3 23.05	-33 40 57.41	-19.808	0.824	2.165		
13	HD 98069	8.16	11 16 44.62	-3 56 34.57	-0.435	-4.224	3.420	55.24	16148.71
	UCAC4 431-054639	11.18	11 16 48.07	-3 56 54.40	-0.331	-4.303	3.286		
14	HD 94390	8.96	10 53 7.81	-44 49 13.53	-15.059	-1.990	3.737	7.98	2136.26
	Gaia DR3 5387858145792881152		10 53 8.56	-44 49 14.24	-14.327	-2.293	3.713		
15	HD 162193	8.66	17 53 33.95	-59 42 25.73	1.441	-15.944	3.549	15.28	4305.24
	Gaia DR3 5917808942063785088		17 53 34.53	-59 42 40.36	1.896	-15.852	3.569		
16	HD 223352	4.57	23 48 55.67	-28 7 50.68	99.435	-106.240	22.730	74.71	3287.04
	HD 223340	9.28	23 48 50.61	-28 7 17.35	96.589	-105.274	22.682		
17	HD 94326	7.76	10 52 33.30	-46 13 1.95	-24.595	8.099	3.426	40.31	11766.79
	Gaia DR3 5363470118895488512		10 52 32.35	-46 13 41.04	-24.233	8.412	3.563		
18	BD-15 4515	9.97	17 19 12.91	-15 54 37.47	4.679	0.519	3.064	62.43	20374.60
	Gaia DR3 4136170951949470464		17 19 10.80	-15 55 31.96	4.725	0.211	3.028		
19	HD 34799	8.23	5 18 46.06	-28 52 20.98	3.349	-15.314	4.291	20.72	4829.66
	Gaia DR3 2954518486936209792		5 18 45.12	-28 52 4.34	3.262	-15.948	4.150		

Table 2. Magnitudes and astrometric data for the stars studied in this work.

Star	V	α	δ	μ_α	μ_δ	π	Spectra	S/N @5000 Å
		J2000	J2000	[mas/yr]	[mas/yr]	[mas]		
HD 87304	9.49	10 03 23.43	-33 41 02.58	-19.776	0.833	2.204	Gemini+GHOST	275
CD-33 6615B	12.60	10 03 23.05	-33 40 57.41	-19.808	0.824	2.165	Gemini+GHOST	220
HD 98069	8.16	11 16 44.62	-3 56 34.57	-0.435	-4.224	3.420	CASLEO+REOSC	350
UCAC4 431-054639	11.18	11 16 48.07	-3 56 54.40	-0.331	-4.303	3.286	CASLEO+REOSC	170
HD 153747	7.42	17 02 53.84	-38 27 36.60	7.488	13.836	5.647	CASLEO+REOSC	300
TYC 7869-2003-1	11.84	17 02 38.75	-38 23 07.05	7.604	13.963	5.627	CASLEO+REOSC	130

3. Stellar parameters and abundance analysis

Stellar parameters were determined as homogeneously as possible for the stars in our sample, including both late-type and early-type stars. We used the Virtual Observatory Sed Analyzer⁴ (VOSA, Bayo et al. 2008) and the spectral energy distributions (SEDs) constructed from photometric data, to obtain the stellar effective temperatures (T_{eff}) of the objects in our sample via atmospheric model fitting. Observed SEDs were unreddened by VOSA using the extinction maps of Schlegel et al. (1998) and following the procedure of Bilir et al. (2008) to derive A_V . We used a grid of Kurucz-NEWODF models by Kurucz (1993) covering T_{eff} between 3500 K and 13000 K with a step of 250 K. Then, we performed a Bayesian estimation of surface gravities $\log g$ using Gaia eDR3 parallaxes with the PARAM 1.3 interface⁵ (da Silva et al. 2006). Temperatures and gravities derived for the stars in our sample are presented in the Table 3.

Projected rotational velocities $v \sin i$ were first estimated by fitting the line Mg II 4481.23 Å and then refined by fitting most Fe I and Fe II lines in the spectra. Synthetic spectra were calculated using the program SYNTH (Kurucz & Avrett 1981) together with ATLAS12 (Kurucz 1993) model atmospheres, and then convolved with a rotational profile (using the Kurucz's command *rotate*) and with an instrumental profile for each spectrograph (using the command *broaden*). The resulting $v \sin i$ values are shown in the 6th column of Table 3, covering between $10.3 \pm 0.2 \text{ km s}^{-1}$ and $140.5 \pm 3.6 \text{ km s}^{-1}$ for the stars in our sample. Microturbulence velocity v_{micro} was estimated as a function of T_{eff} following the formula of Gebran et al. (2014), which is valid for $\sim 6000 \text{ K} < T_{\text{eff}} < \sim 10000 \text{ K}$. We adopted an uncertainty of $\sim 25\%$ for v_{micro} , as suggested by Gebran et al. (2014), and then this uncertainty was taken into account in the abundance error calculation.

We applied an iterative procedure to determine the chemical abundances for the stars in our sample. As a first step, we computed an ATLAS12 (Kurucz 1993) model atmosphere, adopting initially solar abundances from Asplund et al. (2009). The

⁴ <http://svo2.cab.inta-csic.es/theory/vosa/>

⁵ http://stev.oapd.inaf.it/cgi-bin/param_1.3

Table 3. Fundamental parameters derived for the stars in this work.

Star	T_{eff} [K]	$\log g$ [dex]	[Fe/H] [dex]	v_{micro} [km s ⁻¹]	$v \sin i$ [km s ⁻¹]
HD 87304	7750 \pm 250	3.85 \pm 0.06	-1.17 \pm 0.14	3.21 \pm 0.80	140.5 \pm 3.6
CD-33 6615B	6250 \pm 250	4.34 \pm 0.06	-0.05 \pm 0.15	1.02 \pm 0.25	13.7 \pm 0.7
HD 98069	7500 \pm 250	3.67 \pm 0.06	-1.05 \pm 0.13	3.00 \pm 0.75	80.5 \pm 2.1
UCAC4 431-054639	6000 \pm 250	4.17 \pm 0.09	-0.16 \pm 0.17	0.68 \pm 0.17	21.0 \pm 0.8
HD 153747	9250 \pm 250	4.14 \pm 0.04	-0.94 \pm 0.16	2.37 \pm 0.59	82.1 \pm 2.7
TYC 7869-2003-1	5750 \pm 250	4.50 \pm 0.03	+0.00 \pm 0.15	0.42 \pm 0.11	10.3 \pm 0.2

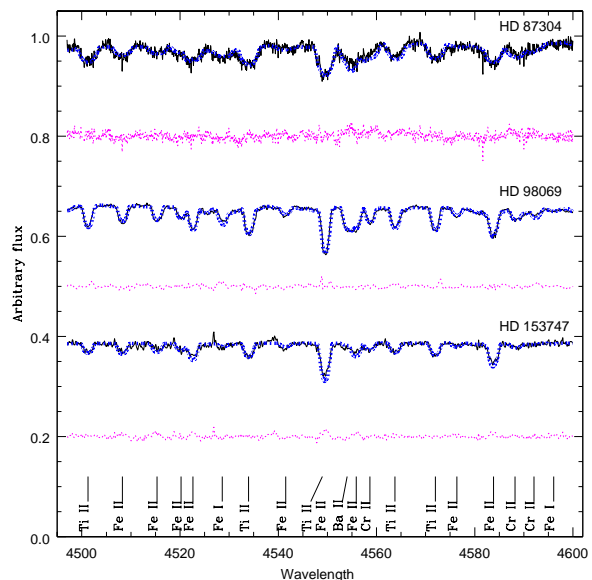
corresponding abundances were then obtained by fitting the observed spectra with the program SYNTHE (Kurucz & Avrett 1981). With the new abundance values, we derived a new model atmosphere and restarted the process again. In each step, opacities were calculated for an arbitrary composition and v_{micro} using the opacity sampling (OS) method, similar to previous works (Saffe et al. 2020, 2021, 2022; Alacoria et al. 2022). In this way, parameters and abundances were consistently derived using specific opacities rather than solar-scaled values, until reach the same input and output abundances (for more details, see Saffe et al. 2021). Possible differences originating from the use of solar-scaled opacities instead of an arbitrary composition were recently estimated for solar-type stars (Saffe et al. 2018, 2019). These differences could become particularly important when modeling chemically peculiar stars, where solar-scaled models could result in a very different atmospheric structure (e.g., Piskunov & Kupka 2001) and reach abundance differences up to 0.25 dex (Khan & Shulyak 2007).

We derived the chemical abundances for 31 different species, including Li I, C I, O I, Na I, Mg I, Mg II, Al I, Si I, Si II, S II, Ca I, Ca II, Sc I, Sc II, Ti I, Ti II, V I, Cr I, Cr II, Mn I, Fe I, Fe II, Co I, Ni I, Cu I, Zn I, Sr II, Y II, Ba II, La II and Ce II. The atomic line list and laboratory data used in this work are the same described in Saffe et al. (2021). Figure 1 presents an example of observed, synthetic, and difference spectra (black, blue dotted, and magenta lines) for some stars in our sample. There is a good agreement between the results of modeling and the observations for the lines of different chemical species.

The uncertainty in the abundance values was estimated considering different sources. We estimated the measurement error, e_1 , from the line-to-line dispersion as σ/\sqrt{n} , where σ is the standard deviation and n is the number of lines. For elements with only one line, we adopted for σ the standard deviation of the iron lines. Then, we determined the contribution to the abundance error due to the uncertainty in stellar parameters. We modified T_{eff} , $\log g$, and v_{micro} by their uncertainties and recalculated the abundances, obtaining the corresponding differences e_2 , e_3 , and e_4 (we adopt a minimum of 0.01 dex for these errors). Finally, the total error e_{tot} was estimated as the quadratic sum of e_1 , e_2 , e_3 , and e_4 . The abundances with their total error e_{tot} , the individual errors e_1 to e_4 , and the number of lines n , are presented in the Tables A.1 to A.6 of the Appendix.

3.1. NLTE effects

In the case of λ Boo stars, light-element non-local thermodynamic equilibrium (NLTE) abundances are particularly important. For example, an average O I correction of -0.5 dex was derived by Paunzen et al. (1999) for a sample of λ Boo stars; while for C I, they estimated an average correction of -0.1 dex. Rentzsch-Holm (1996) derived neutral carbon NLTE abundance corrections by using a multilevel model atom for stars with T_{eff}


Fig. 1. Observed, synthetic, and difference spectra (black, blue dotted, and magenta lines) for some stars in our sample.

between 7000 K and 12000 K, $\log g$ between 3.5 and 4.5 dex, and metallicities from -0.5 dex to +1.0 dex. She showed that C I NLTE effects are negative (calculated as NLTE-LTE) and depend basically on equivalent width W_{eq} . Near \sim 7000 K, the three lower levels of C I are always in LTE; however, increasing the T_{eff} values increases the underpopulation of these levels respect to LTE by UV photoionization. Thus, we estimated NLTE abundance corrections of C I for the early-type stars in our sample by interpolating in their Figs. 7 and 8 as a function of T_{eff} , W_{eq} , and metallicity. We applied a similar correction in previous works (Alacoria et al. 2022), which allows the comparison of abundance values.

NLTE abundance corrections for O I were derived by Sitnova et al. (2013), who used a multilevel model atom with 51 levels. The authors showed that NLTE effects lead to a strengthening of O I lines, producing a negative NLTE correction. They calculated NLTE corrections for a grid of model atmospheres, including stars with spectral types from A to K (T_{eff} between 10000 and 5000 K). We estimated NLTE abundance corrections of O I (IR triplet 7771 Å) for the stars in this work, interpolating based on Table 11 of Sitnova et al. (2013), as a function of T_{eff} . We note that other O I lines present corrections lower than \sim -0.02 dex (see, e.g., Table 5 of Sitnova et al. 2013).

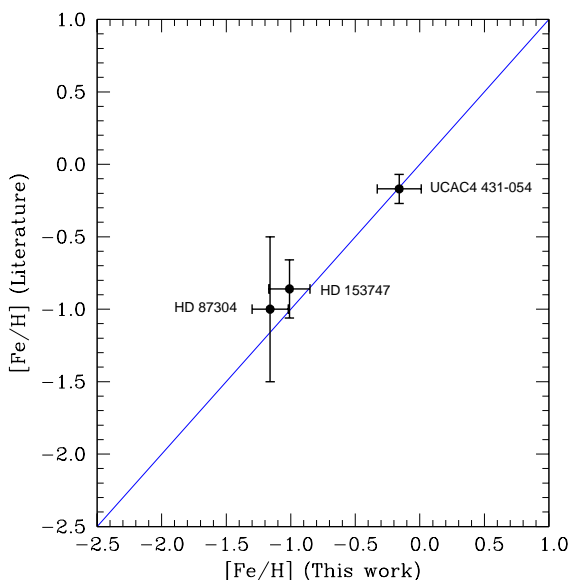


Fig. 2. Comparison of $[\text{Fe}/\text{H}]$ values derived in this work with those from literature.

3.2. Comparisons with the literature

We present in Fig. 2 a comparison of $[\text{Fe}/\text{H}]$ values derived in this work, with those taken from literature for the stars UCAC4 431-054639 (Steinmetz et al. 2020), HD 87304 (Gray et al. 2017) and HD 153747 (Pauzen et al. 2002b). In general, there is a good agreement with the literature. The two stars with the lowest metallicity (HD 87304 and HD 153747) seem to present literature values slightly higher than in the present work. However, the values could still be considered similar within their error bars.

4. Discussion

We discuss in this section the chemical composition of the binary systems, which include a candidate λ Boo star and a late-type companion. The chemical patterns of the early-type stars are compared to an average pattern of λ Boo stars. We caution that to derive an average pattern for λ Boo stars is not an easy task, due to the relatively low number of stars homogeneously analyzed (see e.g. Section 4.1 of Alacoria et al. 2022). We use in this work the same average chemical pattern of Alacoria et al. (2022). Basically, we adopt the data derived by Heiter et al. (2002), who homogeneously determined abundances for a number of λ Boo stars, and then we excluded from the average those stars without CNO values, similar to Alacoria et al. (2022).

4.1. Binary system HD 87304 + CD-33 6615B

The star HD 87304 was classified by Gray et al. (2017) as A8 V kA2.5mA2.5 λ Boo. However, the authors caution that the identification as member of the λ Boo class should be followed up with high-resolution abundance studies to confirm a λ Boo abundance pattern, similar to the present work. The candidate λ Boo star HD 87304 is accompanied by CD-33 6615B, a late-type star separated by 6.97 arcsec or 3160.67 au (El-Badry et al. 2021). El-Badry et al. (2021) estimated empirically a probability that each pair is a chance alignment (R in their paper and "R_chance_align" in their catalog). The authors consider "high

bound probability" or "high confidence" pairs those with $R < 0.1$, corresponding to $> 90\%$ probability of being bound. In particular, this pair presents $R = 1.24 \cdot 10^{-4}$, being considered as a high bound probability pair. The separation allows us to analyze both stars independently without contamination from its companion, which is different than other λ Boo stars (see e.g. Pauzen et al. 2012a,b). To our knowledge, there is no detailed abundance determination for any component of this binary system.

We note that the Li abundance is significantly supersolar in CD-33 6615B ($[\text{Li}/\text{H}] = 1.72 \pm 0.22$ dex). We present in Fig. 3 a spectral region near the Li line 6707.8 Å in this star. Observed and synthetic spectra are shown with black and blue dotted lines. For the synthetic lines, the plot indicates the wavelength, atomic number, and intensity (between 1 and 0). The lithium line 6707.8 Å was detected in CD-33 6615B but not in their companion HD 87304 (which is a λ Boo star, as we will see below). Interestingly, for the case of the triple system HD 15615, the Li line was detected in the early-type star HD 15164 (see Fig. 5 in Alacoria et al. 2022) but not in their λ Boo companion HD 15165. However, we caution that lithium abundance is sensitive to different effects, probably not related to the λ Boo peculiarity. For example, there is a known correlation between lithium content and age. Moreover, its abundance depends on other factors such as metallicity in solar-type stars (see, for example, Fig. 3 of Martos et al. 2023) or even the possible engulfment of a rocky planet (Saffe et al. 2017; Soares et al. 2025). We therefore consider that lithium content deserves to be further explored with a larger sample of stars.

We present in Fig. 4 the chemical pattern of the stars CD-33 6615B and HD 87304 (left and right panels), compared to an average pattern of λ Boo stars (blue). For each star, we present two panels, corresponding to elements with atomic number $z < 32$ and $z > 32$. The error bars of the λ Boo pattern show the standard deviation derived from different stars, while the error bars for our stars correspond to the total error, e_{tot} . From Fig. 4, the different chemical composition of both stars is striking. On one side, CD-33 6615B presents mostly a solar chemical pattern (for instance, $[\text{Fe}/\text{H}] = -0.05 \pm 0.15$ dex), with some elements above solar values (Y, Ba and La). In particular, the light elements C, O and S present solar abundances.

On the other hand, HD 87304 presents a chemical pattern that agrees with those of λ Boo stars (see Fig. 4). For instance, C and O present solar or slightly subsolar values ($[\text{C}/\text{H}] = -0.15 \pm 0.16$ dex, $[\text{O}/\text{H}] = -0.24 \pm 0.27$ dex), which is similar to other λ Boo stars. Other metals such as Ca, Ti and Fe, present abundances ~ 1 dex below solar values. The abundance values confirm the bona fide λ Boo nature of this object. Interestingly, although C and O are almost solar in HD 87304, they seem to be slightly lower than in CD-33 6615B ($[\text{C}/\text{H}] = -0.03 \pm 0.17$ dex, $[\text{O}/\text{H}] = -0.01 \pm 0.17$ dex). This would suggest that, perhaps, the λ Boo phenomena also slightly modifies light element abundances (in addition to a stronger effect on heavier species); however, we caution that NLTE effects could play a role in light elements. Other metals present a significant difference between both stars (for example, Fe differs by $\Delta[\text{Fe}/\text{H}] \sim 1.12 \pm 0.21$ dex). This is one of the highest differences in metallicity found between two stars in a binary system (see, for example, Saffe et al. 2017, 2022).

In summary, this binary system is composed by a late-type star with mostly a solar-like composition, and an early-type object with a λ Boo chemical pattern. This pair shows that λ Boo stars are born with a very different composition, approximately solar, and reinforces the idea that λ Boo stars are Population I ob-

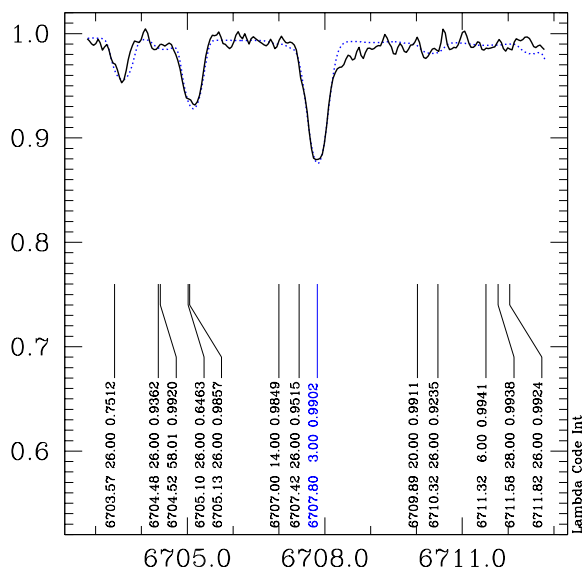


Fig. 3. Observed spectra (black line) and synthetic spectra (blue dotted line) near the Li line 6707.8 Å in the star CD-33 6615B. Synthetic lines are indicated showing the wavelength, atomic number, and intensity.

jects. A similar result was obtained by studying the triple system HD 15165 (Alacoria et al. 2022), the only system reported (up to now) which includes a late-type star with solar-like composition (HD 15165C) and a λ Boo companion (HD 15165). This is the most likely result of the analysis, however, we caution that other explanations are also possible (we will come back to this point in section 4.4).

4.2. Binary system HD 98069 + UCAC4 431-054639

The star HD 98069 was classified as A9 V kA2mA2 (λ Boo) by Murphy et al. (2020). Interestingly, the K2 (Kepler-2) light curve revealed its δ Scuti nature, with eighth pulsation peaks exceeding 1 mmag and seven peaks exceeding 0.05 mmag (Murphy et al. 2020,b). This candidate λ Boo star (HD 98069) is accompanied by UCAC4 431-054639, a late-type star separated by 55.24 arcsec or 16148.71 au (El-Badry et al. 2021). This binary presents a chance alignment probability of $R=1.24 \cdot 10^{-4}$, being considered as a high bound probability pair (El-Badry et al. 2021). The separation allows us to analyze both stars independently without contamination from its companion. To our knowledge, there is no detailed abundance determination for HD 98069.

We present in Fig. 5 the chemical pattern of the stars UCAC4 431-054639 and HD 98069 (left and right panels), compared to an average pattern of λ Boo stars. The symbols of Fig. 5 are similar to those used in the Fig. 4. It is clear from Fig. 5 that both stars present a significantly different chemical pattern, similar to the previous binary system. On one side, UCAC4 431-054639 presents mostly a solar chemical pattern within $\pm \sim 0.20$ dex, with some species showing slightly subsolar (Mg, Sc, Fe) or slightly supersolar (Ca, Y) abundance values. For example, for iron we obtained $[\text{Fe}/\text{H}]=-0.16 \pm 0.17$ dex, while light-element abundances (CNOS) were not derived.

On the other hand, the chemical pattern of HD 98069 is very different than its stellar companion (see Fig. 5, right panel). C displays an abundance close to solar, or slightly subsolar ($[\text{C}/\text{H}]=-0.21 \pm 0.05$). Most species are strongly depleted com-

pared to the solar values by ~ 1 dex or more (Al, Ca, Ti, Cr, Fe), except perhaps Si which is less depleted ($[\text{Si}/\text{H}]=-0.37 \pm 0.22$ dex). However, we caution that the Si abundance was derived using only one line. Then, the general pattern of HD 98069 seems to agree with those of λ Boo stars. The metallicity of both stars in this binary system differs by $\Delta[\text{Fe}/\text{H}] \sim 0.89 \pm 0.21$ dex, which is also significant although a less extreme difference than the previous binary system.

In summary, this binary system is composed by a late-type star with mostly a solar-like composition, and an early-type object with a λ Boo-like chemical pattern.

4.3. Binary system HD 153747 + TYC 7869-2003-1

The star HD 153747 was classified by Paunzen et al. (2001b) as hA7mA0 V λ Boo, and later as A7 V kA0mA0 λ Boo by Murphy et al. (2015), who discussed the membership of this object to the λ Boo class. This object is also reported as λ Boo in other literature works (Gray et al. 2017; Murphy et al. 2020). Desikachary & McInally (2014) reported multiperiodicity (periods between 0.96 and 1.2 h) in the light curve of HD 153747, while Paunzen et al. (2001b) noted their δ Sct variability. For this star, Paunzen et al. (2002b) reported a depleted metal content of $[\text{Z}/\text{H}]=-0.86 \pm 0.20$ dex, estimated using Δm_2 from the Geneva 7-color as well as Δm_1 from the uvby β photometric system. This candidate λ Boo star (HD 153747) is accompanied by TYC 7869-2003-1, a late-type star separated by 322.64 arcsec or 57131.24 au (El-Badry et al. 2021). This pair presents a chance alignment probability of $R=0.0885$, somewhat higher than previous binary systems, although it is still considered as a high bound probability pair (El-Badry et al. 2021). The separation allows us to analyze both stars independently without contamination from its companion. To our knowledge, there is no detailed (spectroscopic) abundance determination for any component of this binary system.

We present in Fig. 6 the chemical pattern of the stars TYC 7869-2003-1 and HD 153747 (left and right panels), compared to an average pattern of λ Boo stars. The symbols of Fig. 6 are similar to those used in Figs. 4 and 5. Both stars present a significantly different chemical pattern, similar to previous binary systems. TYC 7869-2003-1 displays mostly a solar chemical pattern, while HD 153747 presents a chemical pattern which closely follows the average pattern of λ Boo stars. HD 153747 displays nearly solar C and O abundances ($[\text{C}/\text{H}]=0.09 \pm 0.12$ dex, $[\text{O}/\text{H}]=-0.18 \pm 0.16$ dex), while other metals show strong depletions of ~ 1 dex (for example, $[\text{Fe}/\text{H}]=-0.94 \pm 0.16$ dex). The metallicity of both stars in this binary system differs by $\Delta[\text{Fe}/\text{H}] \sim 0.94 \pm 0.22$ dex.

In summary, this binary system is composed by a solar-composition late-type star, and a λ Boo early-type star.

4.4. The relevance of λ Boo stars with late-type companions

We discuss in this section the importance of finding λ Boo stars accompanied by late-type stars. For the first time, we studied binary systems composed by a late-type object and a candidate λ Boo star. Different authors note that the identification of λ Boo stars (starting with candidates suggested by spectral classification) should be followed up with a high-resolution abundance analysis to confirm their λ Boo nature (see e.g. Andrievsky et al. 2002; Heiter et al. 2002; Murphy et al. 2015; Gray et al. 2017; Alacoria et al. 2022). In this work, we applied a similar procedure and confirmed the λ Boo membership of three early-type

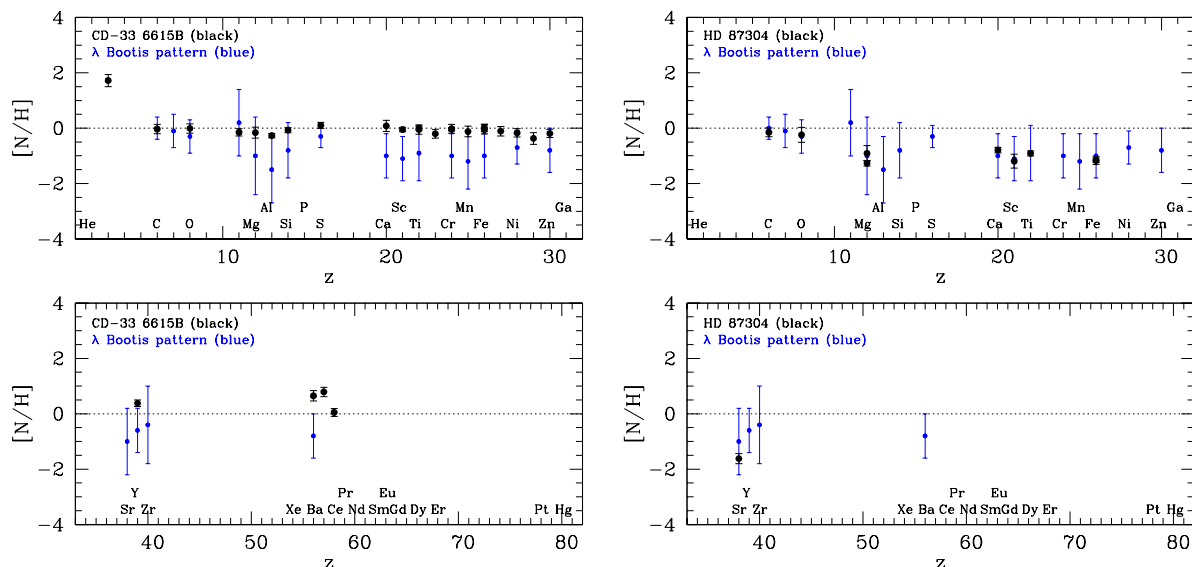


Fig. 4. Chemical pattern of the stars CD-33 6615B and HD 87304 (left and right panels), compared to an average pattern of λ Boo stars (blue).

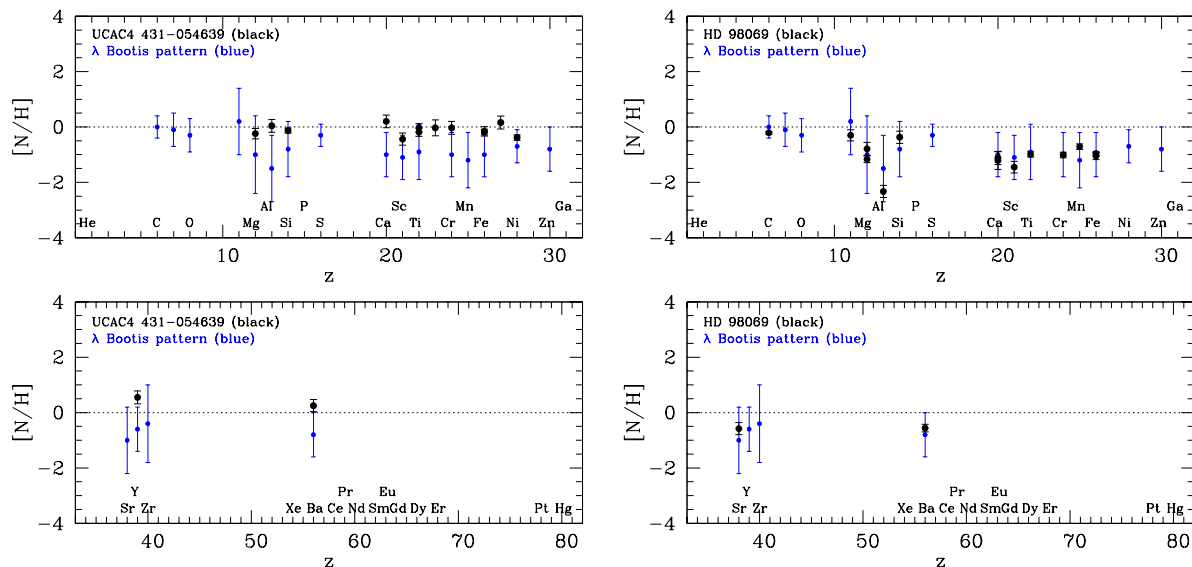


Fig. 5. Chemical pattern of the stars UCAC4 431-054639 and HD 98069 (left and right panels), compared to an average pattern of λ Boo stars (blue).

stars (HD 87304, HD 98069 and HD 153747), as we can see in the Figs. 4, 5 and 6. These three stars could be then considered as bona fide λ Boo stars.

We also showed that the late-type companions that belong to these binary systems present mostly a solar-like composition. This composition could be used as a proxy for the initial composition of the material from which the λ Boo star formed (under the hypothesis that they are born from the same molecular cloud). To our knowledge, the starting solar-like composition was only showed in the triple system HD 15165 (Alacoria et al. 2022), giving us the opportunity to strengthen this result in the present work. This is an important constraint for any model attempting to explain the λ Boo phenomena. Most scenarios trying to explain the λ Boo stars usually assume a starting solar-like composition (e.g. Martinez-Galarza et al. 2009; Jura 2015). The present work provides three numerical examples of possi-

ble "starting" and "ending" compositions, which could be further explored to test and constraint numerically formation models of λ Boo stars.

In addition, the solar-like composition of the late-type stars is in agreement with the idea that λ Boo stars are Population I objects. For example, Paunzen et al. (2014) concluded that it is possible to distinguish λ Boo stars from intermediate Population II stars on the basis of elemental abundances, though not in terms of kinematics. The authors suggest to use binary systems to strengthen the conclusion that λ Boo stars are a distinct population from the Population II group. The results of the present work support the idea that λ Boo stars belong to Population I, in agreement with Paunzen et al. (2014). This is the most likely result of the analysis, however, we caution that other explanations are also possible. For example, we mentioned that 15% of A-type stars have companions with periods of 100-1500

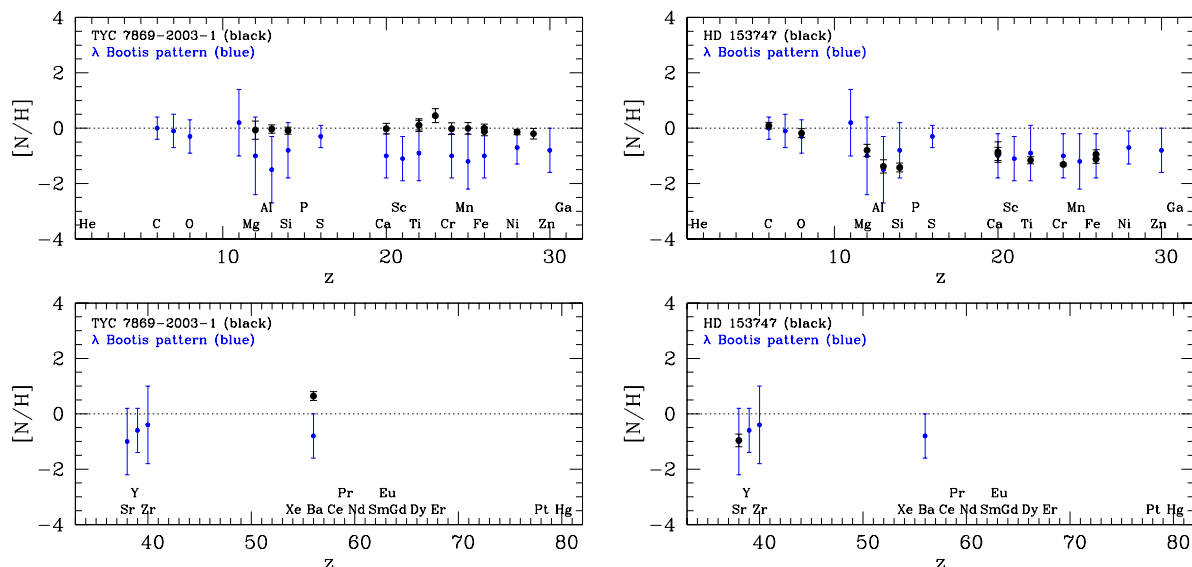


Fig. 6. Chemical pattern of the stars TYC 7869-2003-1 and HD 153747 (left and right panels), compared to an average pattern of λ Boo stars (blue).

days (Murphy et al. 2018) which would be undetected in the El-Badry et al. (2021) study. Furthermore, 21% of those companions are white dwarfs (WDs). Perhaps, the λ Boo star once had a tight orbit with a higher-mass companion that became a red giant, transferred mass, and is now an undetected WD, such as those suggested by Murphy et al. (2018). For example, Van Winckel et al. (1995) presented five extremely Fe-deficient post-AGB binary systems with orbital periods from one to a few years, suggesting that mass transfer has occurred in these systems. Paunzen et al. (1998) suggested that a similar mass-transfer might also be an additional mechanism to be considered for the λ Boo phenomenon. Then, in our binary systems, the cool star could have been captured by the hypothetical tight binary and be of any age.

In general, the present results are in agreement with those previously obtained in the triple system HD 15165 (Alacoria et al. 2022), in which a λ Boo star (HD 15165) is accompanied by a late-type star with solar-like composition (HD 15165C). To our knowledge, λ Boo stars were detected in binary (and multiple) systems accompanied by early-type stars (e.g. Paunzen et al. 2012a,b; Alacoria et al. 2022), by late-type companions (this work and Alacoria et al. 2022), and even one case accompanied by a Brown Dwarf (ζ Del, detected by Saffe et al. 2021). However, no bona fide λ Boo star have been detected in open clusters (e.g. Paunzen et al. 2001a,b; Gray & Corbally 2002), including searches in different intermediate-age open clusters. Other chemically peculiar stars (such as Am or Ap) were detected in the same clusters (e.g. Gray & Corbally 2002). It would be valuable to detect λ Boo stars in open clusters, which could also be used to study their origin.

The work of Jura (2015) mentioned the possibility that λ Boo stars could originate by accreting the winds from late-type stellar companions (their Section 4.1). Jura (2015) considered that only a small fraction of the material from the late-type stars could reach the λ Boo star and then ruled out this scenario (instead, the author proposed winds from hot-Jupiter planets as a plausible mechanism). In the present work, we analyzed binary systems including λ Boo stars and late-type companions. However, the three binary systems analyzed here present wide separa-

tions (from 3160 au to 57131 au, see Table 1), making unlikely the suggested mechanism. On the other hand, there are no planets reported orbiting the λ Boo stars studied in this work.

5. Concluding remarks

In the present work, we cross-matched an homogeneous list of candidate λ Boo stars with a recent catalog of resolved binaries detected with Gaia eDR3, with the aim of finding λ Boo stars as members of multiple systems. Then, we performed a detailed abundance determination of three of these binary systems. The main results of this work are as follows:

- We present a group of 19 newly identified binary systems that contains a candidate λ Boo star (see Table 1). The new systems allow to ~duplicate the number of λ Boo stars currently known in multiple systems. This important group could be used in further studies of λ Boo stars.

- For the first time, we performed a detailed abundance analysis of three binary systems including a candidate λ Boo star and a late-type companion. We confirmed the true λ Boo nature of the three early-type stars, and obtained mostly a solar-like composition for the late-type components. In particular, the binary system HD 87304 + CD-33 6615B presents a mutual metallicity difference of $\Delta[\text{Fe}/\text{H}] \sim 1.12 \pm 0.21$ dex, one of the highest differences found in a binary system.

- Adopting as a proxy the chemical composition of the late-type stars, we showed that the three λ Boo stars were initially born with a solar-like composition. This is an important constraint for any scenario trying to explain the origin of λ Boo stars. The present work provides three numerical examples of possible "starting" and "ending" compositions to test the models.

- Finally, the solar-like composition of the late-type stars supports the idea that λ Boo stars are Population I objects. This is in agreement with the suggestions of previous works (Paunzen et al. 2014; Alacoria et al. 2022). However, we caution that other explanations are also possible.

The present work shows the importance of finding λ Boo stars that belong to multiple systems. The stars used in this work correspond mostly to southern λ Boo stars. We encourage to per-

form a similar work on additional binary systems, and to expand the list of homogeneous λ Boo candidates to the North hemisphere.

Acknowledgements. We thank the referee for constructive comments that improved the paper. The authors thank Dr. R. Kurucz for making their codes available to us. CS acknowledge financial support from CONICET (Argentina) through grant PIP 11220210100048CO and the National University of San Juan (Argentina) through grant CICITCA 21/E1235. IRAF is distributed by the National Optical Astronomical Observatories, which is operated by the Association of Universities for Research in Astronomy, Inc., under a cooperative agreement with the National Science Foundation. Based on data acquired at Complejo Astronómico El Leoncito, operated under agreement between the Consejo Nacional de Investigaciones Científicas y Técnicas de la República Argentina and the National Universities of La Plata, Córdoba and San Juan.

References

- Alacoria, J., Saffe, C., Jaque Arancibia, M., et al., 2022, *A&A* 660, A98
 Andrievsky, S., Chernyshova, I., Paunzen, E., et al., 2002, *A&A* 396, 641
 Asplund, M., Grevesse, N., Sauval, A., Scott, P., 2009, *ARA&A* 47, 481
 Bayo, A., Rodrigo, C., Barrado y Navascués, D., et al., 2008, *A&A* 492, 277
 Bilir, S., Soyduğan, E., Soyduğan, F., Yaz, E., et al., 2008, *AN* 329, 835
 Cowley, C. R., Sears, R. L., Aikman, G., Sadakane, K., 1982, *AJ* 254, 191
 da Silva, L., Girardi, L., Pasquini, L., et al., 2006, *A&A* 458, 609
 Desikachary, K., McNally, C. J. 1979, *MNRAS*, 188, 67
 Gebran, M., Monier, R., Royer, F., Lobel, A., Blomme, R., 2014, *Putting A Stars into Context: Evolution, Environment, and Related Stars*, Proceedings of the international conference held on June 3-7, 2013 at Moscow M.V. Lomonosov State University in Moscow, Russia. Eds.: G. Mathys, E. Griffin, O. Kochukhov, R. Monier, G. Wahlgren, Moscow: Publishing house "Pero", 2014, p. 193-198
 Gray, R. O. 1988, *AJ*, 95, 220
 Gray, R. O., Corbally, C. J., 1998, *AJ* 116, 2530
 Gray, R. O., Corbally, C. J., 2002, *AJ* 124, 989
 Gray, R., Riggs, Q., Koen, C., et al., 2017, *AJ* 154, 31
 Heiter, U., 2002, *A&A* 381, 959
 Jura, M., 2015, *AJ* 150, 166
 Kama, M., Folsom, C. P., Pinilla, P., 2015, *A&A* 582, L10
 Kamp, I., Iliev, I. Kh., Paunzen, E., et al., 2001, *A&A* 375, 899
 Kamp, I., Paunzen, E., 2002, *MNRAS* 335, L45
 Khan, S., Shulyak, D., 2007, *A&A* 469, 1083
 Kunitomo, M., Guillot, T., Ida, S., Takeuchi, T., 2018, *A&A* 618, A132
 Kurucz, R. L. 1993, *ATLAS9 Stellar Atmosphere Programs and 2 km/s grid*, Kurucz CD-ROM 13 (Cambridge, MA: Smithsonian Astrophysical Obs.)
 Kurucz, R. L., Avrett, E. H., 1981, *SAO Special Report No. 391*
 Martínez-Galarza, J., Kamp, I., Su, K. Y., et al. 2009, *ApJ*, 694, 165
 Martos, G., Meléndez, J., Rathsam, A., et al., 2023, *MNRAS* 522, 3217
 Murphy, S., Corbally, C., Gray, R., et al., 2015, *PASA* 32, e036
 Murphy, S., Moe, M., Kurtz, D., Bedding, T., Shibahashi, H., Boffin, H., 2018, *MNRAS* 474, 4322
 Murphy, S., Gray, R., Corbally, C., et al., 2020, *MNRAS* 499, 2701
 Murphy, S., Paunzen, E., Bedding, T. R., et al., 2020, *MNRAS* 495, 1888
 Murphy, S. J., Paunzen, E., 2017, *MNRAS* 466, 546
 El-Badry, K., Rix, H.-W., Heintz, T., 2021, *MNRAS* 506, 2269
 Paunzen, E., Heiter, U., Handler, G., et al., 1998, *A&A* 329, 155
 Paunzen, E., Kamp, I., Iliev, I. Kh., et al., 1999, *A&A* 345, 597
 Paunzen, E., Duffee, B., Heiter, U., et al., 2001, *A&A* 373, 625
 Paunzen, E., 2001, *A&A* 373, 633
 Paunzen, E., Handler, G., Weiss, W. W., et al., 2002, *A&A* 392, 515
 Paunzen, E., Fraga, L., Heiter, U., et al., 2012, "From interacting binaries to exoplanets: essential modeling tools", *IAU Proceeding Symposium 282*, M. Richards & I. Hubeny, Eds., doi:10.1017/S1743921311027773
 Paunzen, E., Heiter, U., Fraga, L., et al., 2012, *MNRAS* 419, 3604
 Paunzen, E., Iliev, I., Fossati, L., et al., 2014, *A&A* 567, A67
 Piskunov, N., Kupka, F., 2001, *AJ* 547, 1040
 Rentzsch-Holm, Inga, 1996, *A&A* 312, 966
 Saffe, C., Jofré, E., Martioli, E., et al., 2017, *A&A* 604, L4
 Saffe, C., Flores, M., Miquelarena, P., et al., 2018, *A&A* 620, 54
 Saffe, C., Jofré, E., Miquelarena, P., et al., 2019, *A&A* 625, 39
 Saffe, C., Miquelarena, P., Alacoria, J., et al., 2020, *A&A* 641, 145
 Saffe, C., Miquelarena, P., Alacoria, J., et al., 2021, *A&A* 647, A49
 Saffe, C., Alacoria, J., Miquelarena, P., et al., 2022, *A&A* 668, A157
 Saffe, C., Miquelarena, P., Alacoria, J., et al., 2024, *A&A* 682, L23
 Schlegel, D., Finkbeiner, D. P., Davis, M., 1998, *ApJ* 500, 525
 Sitnova, T., Mashonkina, L., Ryabchikova, T., 2013, *Astronomy Letters*, Vol. 39, No. 2, pp. 126-140
 Soares, B., Adibekyan, V., Mordasini, C., et al., 2025, *A&A* 693, A47
 Steinmetz, M., Guiglion, G., McMillan, P. J., et al., 2020, *AJ* 160, 83
 Stürenburg, S., 1993, *A&A* 277, 139
 Van Winckel, H., Waelkens, C.; Waters, L. B. F. M., 1995, *A&A* 293, L25
 Venn, K., Lambert, D., 1990, *ApJ* 363, 234

Table A.1. Chemical abundances for the star HD 87304.

Species	[X/H] $\pm e_{tot}$	e_1	e_2	e_3	e_4
C I	-0.15 \pm 0.16	0.16	0.01	0.01	0.02
O I	-0.24 \pm 0.27	0.25	0.04	0.01	0.09
Mg I	-1.27 \pm 0.10	0.06	0.07	0.02	0.04
Mg II	-0.91 \pm 0.28	0.25	0.12	0.03	0.03
Ca II	-0.79 \pm 0.10	0.04	0.09	0.01	0.02
Sc II	-1.19 \pm 0.25	0.25	0.05	0.02	0.03
Ti II	-0.91 \pm 0.09	0.04	0.05	0.02	0.05
Fe I	-1.17 \pm 0.14	0.07	0.11	0.01	0.04
Fe II	-1.16 \pm 0.08	0.06	0.04	0.01	0.04
Sr II	-1.62 \pm 0.18	0.05	0.15	0.02	0.08

Table A.2. Chemical abundances for the star CD-33 6615B.

Species	[X/H] $\pm e_{tot}$	e_1	e_2	e_3	e_4
Li I	1.72 \pm 0.22	0.12	0.18	0.01	0.01
C I	-0.03 \pm 0.17	0.02	0.16	0.03	0.01
O I	-0.01 \pm 0.17	0.01	0.16	0.02	0.01
Na I	-0.15 \pm 0.13	0.12	0.04	0.01	0.01
Mg I	-0.16 \pm 0.20	0.10	0.18	0.01	0.01
Al I	-0.27 \pm 0.08	0.04	0.07	0.01	0.01
Si I	-0.07 \pm 0.09	0.05	0.07	0.01	0.01
S I	0.10 \pm 0.11	0.03	0.11	0.02	0.01
Ca I	0.08 \pm 0.20	0.11	0.15	0.01	0.05
Sc II	-0.05 \pm 0.08	0.06	0.03	0.02	0.03
Ti I	-0.05 \pm 0.17	0.03	0.17	0.01	0.01
Ti II	-0.00 \pm 0.07	0.05	0.02	0.02	0.04
V I	-0.20 \pm 0.16	0.09	0.13	0.01	0.02
Cr I	-0.02 \pm 0.16	0.02	0.16	0.01	0.02
Cr II	-0.04 \pm 0.05	0.03	0.02	0.01	0.03
Mn I	-0.12 \pm 0.19	0.12	0.14	0.01	0.05
Fe I	-0.05 \pm 0.16	0.01	0.15	0.01	0.04
Fe II	0.01 \pm 0.14	0.03	0.12	0.01	0.07
Co I	-0.11 \pm 0.17	0.12	0.12	0.01	0.01
Ni I	-0.17 \pm 0.15	0.03	0.14	0.01	0.03
Cu I	-0.37 \pm 0.21	0.12	0.17	0.01	0.01
Zn I	-0.19 \pm 0.15	0.06	0.11	0.01	0.09
Y II	0.38 \pm 0.12	0.12	0.01	0.01	0.01
Ba II	0.65 \pm 0.19	0.12	0.09	0.01	0.12
La II	0.79 \pm 0.17	0.12	0.12	0.02	0.03
Ce II	0.05 \pm 0.14	0.12	0.07	0.02	0.01

Appendix A: Chemical abundances

In this section, we present the chemical abundances and their corresponding errors. The total error e_{tot} was derived as the quadratic sum of the line-to-line dispersion e_1 (estimated as σ/\sqrt{n} , where σ is the standard deviation) and the error in the abundances (e_2 , e_3 , and e_4) when varying T_{eff} , $\log g$, and v_{micro} by their corresponding uncertainties⁶. For chemical species with only one line, we adopted as σ the standard deviation of iron lines. Abundance tables show the average abundance and the total error e_{tot} , together with the errors e_1 to e_4 .

⁶ We adopt a minimum of 0.01 dex for the errors e_2 , e_3 , and e_4 .

Table A.3. Chemical abundances for the star HD 98069.

Species	[X/H] $\pm e_{tot}$	e_1	e_2	e_3	e_4
C I	-0.21 \pm 0.05	0.04	0.04	0.01	0.01
Na I	-0.30 \pm 0.20	0.18	0.08	0.02	0.01
Mg I	-1.17 \pm 0.12	0.06	0.08	0.02	0.07
Mg II	-0.79 \pm 0.23	0.18	0.14	0.02	0.03
Al I	-2.33 \pm 0.22	0.18	0.13	0.01	0.01
Si II	-0.37 \pm 0.22	0.18	0.13	0.02	0.01
Ca I	-1.21 \pm 0.32	0.18	0.21	0.03	0.16
Ca II	-1.12 \pm 0.24	0.18	0.13	0.07	0.04
Sc II	-1.45 \pm 0.21	0.18	0.10	0.01	0.04
Ti II	-0.99 \pm 0.10	0.06	0.04	0.01	0.06
Cr II	-1.01 \pm 0.10	0.10	0.02	0.01	0.01
Mn I	-0.71 \pm 0.10	0.08	0.06	0.01	0.01
Fe I	-1.05 \pm 0.13	0.04	0.11	0.02	0.03
Fe II	-0.96 \pm 0.07	0.05	0.04	0.01	0.03
Sr II	-0.58 \pm 0.22	0.04	0.13	0.01	0.18
Ba II	-0.56 \pm 0.14	0.02	0.13	0.01	0.05

Table A.4. Chemical abundances for the star UCAC4 431-054639.

Species	[X/H] $\pm e_{tot}$	e_1	e_2	e_3	e_4
Mg I	-0.24 \pm 0.19	0.09	0.17	0.01	0.01
Al I	0.04 \pm 0.23	0.20	0.13	0.01	0.01
Si I	-0.13 \pm 0.09	0.07	0.05	0.01	0.01
Ca I	0.20 \pm 0.23	0.12	0.20	0.01	0.03
Sc II	-0.44 \pm 0.22	0.20	0.08	0.03	0.06
Ti I	-0.19 \pm 0.15	0.03	0.14	0.01	0.04
Ti II	-0.03 \pm 0.15	0.06	0.12	0.05	0.03
V I	-0.03 \pm 0.29	0.20	0.21	0.01	0.01
Cr I	-0.03 \pm 0.23	0.11	0.20	0.03	0.05
Fe I	-0.16 \pm 0.17	0.04	0.16	0.01	0.02
Fe II	-0.18 \pm 0.10	0.05	0.07	0.05	0.01
Co I	0.16 \pm 0.23	0.20	0.12	0.01	0.01
Ni I	-0.38 \pm 0.10	0.06	0.08	0.01	0.01
Y II	0.55 \pm 0.23	0.20	0.11	0.03	0.06
Ba II	0.25 \pm 0.22	0.20	0.02	0.03	0.09

Table A.5. Chemical abundances for the star HD 153747.

Species	[X/H] $\pm e_{tot}$	e_1	e_2	e_3	e_4
C I	0.09 \pm 0.12	0.02	0.12	0.01	0.01
O I	-0.18 \pm 0.16	0.16	0.02	0.01	0.01
Mg I	-0.80 \pm 0.22	0.11	0.19	0.01	0.04
Al I	-1.38 \pm 0.24	0.16	0.17	0.01	0.01
Si II	-1.42 \pm 0.16	0.16	0.01	0.01	0.01
Ca I	-0.86 \pm 0.37	0.16	0.33	0.02	0.04
Ca II	-0.93 \pm 0.24	0.16	0.18	0.01	0.01
Ti II	-1.16 \pm 0.13	0.02	0.13	0.01	0.01
Cr II	-1.31 \pm 0.05	0.04	0.02	0.01	0.01
Fe I	-0.94 \pm 0.16	0.04	0.13	0.01	0.08
Fe II	-1.12 \pm 0.15	0.09	0.12	0.01	0.02
Sr II	-0.96 \pm 0.23	0.03	0.23	0.01	0.04

Table A.6. Chemical abundances for the star TYC 7869-2003-1.

Species	$[X/H] \pm e_{tot}$	e_1	e_2	e_3	e_4
Mg I	-0.07 ± 0.33	0.15	0.29	0.01	0.01
Al I	-0.03 ± 0.15	0.15	0.04	0.01	0.01
Si I	-0.09 ± 0.13	0.13	0.01	0.01	0.01
Ca I	-0.02 ± 0.19	0.16	0.11	0.01	0.01
Ti I	0.11 ± 0.17	0.08	0.15	0.01	0.02
Ti II	0.11 ± 0.23	0.22	0.05	0.01	0.01
V I	0.45 ± 0.25	0.08	0.24	0.01	0.01
Cr I	-0.02 ± 0.21	0.15	0.15	0.01	0.02
Mn I	-0.01 ± 0.21	0.13	0.16	0.01	0.01
Fe I	0.00 ± 0.15	0.03	0.14	0.01	0.01
Fe II	-0.12 ± 0.15	0.03	0.15	0.01	0.01
Ni I	-0.14 ± 0.10	0.06	0.07	0.01	0.01
Cu I	-0.20 ± 0.19	0.15	0.11	0.01	0.03
Ba II	0.64 ± 0.16	0.15	0.06	0.01	0.02